

The anticoincidence shield of the PAMELA space experiment

S. Orsi *, P. Carlson, J. Lund, J. Lundquist ¹, M. Pearce

Department of Particle Physics, The Royal Institute of Technology, Albanova University Centre, Stockholm 10691, Sweden

Received 17 September 2004; received in revised form 8 April 2005; accepted 8 May 2005

Abstract

The PAMELA space experiment will be launched in 2005 onboard a Russian Resurs DK1 satellite, orbiting Earth at an altitude varying between 300 and 600 km. The main scientific goal is a study of the antimatter component of the cosmic radiation. The semi-polar orbit (71°) allows PAMELA to investigate a wide range of energies for antiprotons (80 MeV–190 GeV) and positrons (50 MeV–270 GeV). Three years of data taking will provide unprecedented statistics in this energy range and will set the upper limit for the ratio $\bar{H}e/He$ below 10^{-7} . PAMELA is built around a permanent magnet silicon spectrometer, surrounded by a plastic scintillator anticoincidence shield. The anticounter scintillators are used to aid in the rejection of background from particles which do not cleanly enter the acceptance of the experiment but which are responsible for coincidental energy deposits in the trigger scintillators ('false triggers'). Information from the anticounter system can be included as a veto in a second level trigger, to exclude the acquisition of events generated by such false triggers. The construction of the anticounter system is described, along with its functionality and performance. The read-out electronics and the LED-based monitoring system are also described. Test-beam and simulation studies of the system are reviewed.

© 2005 COSPAR. Published by Elsevier Ltd. All rights reserved.

Keywords: Astroparticle physics; Antimatter; Cosmic rays

1. Introduction

PAMELA (a Payload for Antimatter – Matter Exploration and Light – nuclei Astrophysics, PAMELA homepage²; Boezio et al., 2004) is built around a permanent magnet spectrometer (tracker) equipped with double-sided silicon detectors (Adriani et al., 2003). The tracker is surrounded by an anticoincidence (AC) system (Pearce et al., 2003) which can be used to reject particles not cleanly entering PAMELA acceptance. Fig. 1 provides a schematic overview of the host satellite (left), of the PAMELA experiment (centre) and of the AC detectors (right). Above the tracker, the transition radiation detec-

tor (TRD) (Cafagna et al., 2003) is made up of straw-tube detectors interleaved with carbon fibre radiators. The TRD is used to separate electrons and hadrons through threshold velocity measurements. Below the tracker is placed the electromagnetic calorimeter (Boezio et al., 2002), which consists of silicon strip detectors interleaved with tungsten absorber planes ($\lambda = 0.6$, $X_0 = 16.3$). Its main aim is the energy measurement of electrons and positrons. It is also used for particle identification by distinguishing between electromagnetic and hadronic showers. The bottom scintillator (S4) and the neutron detector are placed below the calorimeter and measure highly energetic events not contained in the calorimeter, aiding separation between electromagnetic and hadronic showers. The Time of Flight System (ToF) (Campana et al., 2003) consists of three groups of scintillators (S1–S3). It measures the velocity of the incident particles, rejecting albedo (up-going) particles, and acts as the main PAMELA trigger (Osteria et al., 2004) by coincidence of

* Corresponding author. Tel.: +46 855378187; fax: +46 855378216.

E-mail address: silvio@particle.kth.se (S. Orsi).

¹ Present address: INFN Laboratories, via A. Valerio 2, 34127 Trieste, Italy.

² <http://wizard.roma2.infn.it/pamela/>.

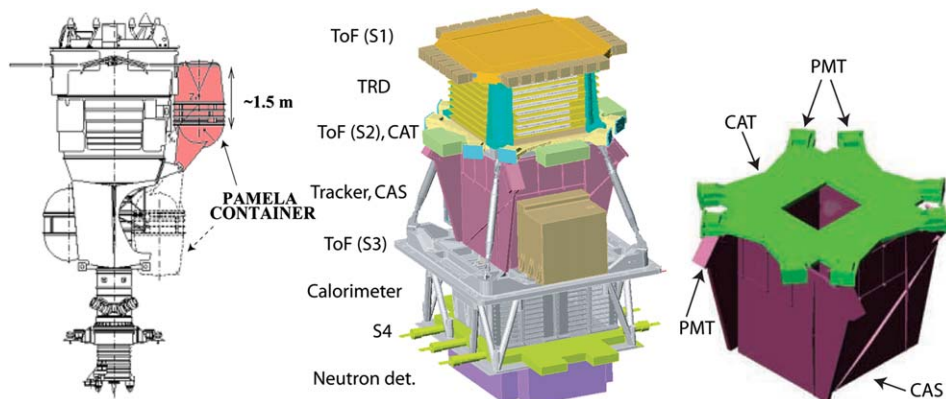


Fig. 1. (Left) The Resurs-DK1 satellite weighs ~ 10 ton. (Centre) The PAMELA experiment is ~ 1.2 m high and weighs ~ 450 kg (750 kg with its container). (Right) The anticoincidence system is ~ 0.4 m high and weighs ~ 16 kg.

energy deposits in the scintillators. A detailed description of the PAMELA apparatus is presented in Boezio et al. (2004). In order to increase the PAMELA geometrical acceptance for electrons at energies above 300 GeV, a self-trigger feature is implemented in the calorimeter. Simulations (Lund, 2002) have shown that the majority of triggers in space are expected to be ‘false triggers’, i.e., where the coincidental energy deposits in the ToF scintillators are generated by secondary particles, produced in the mechanical structure of the experiment. The false trigger rate is expected to be 17.0 Hz (2.8 Hz) in the polar (equatorial) region. The good-trigger rate in the polar (equatorial) region is expected to be 7.2 Hz (0.3 Hz). The AC shields will help identify these ‘false-trigger’ events and reject them during off-line data analysis. Some of the ‘good-triggers’, i.e., events characterised by one particle cleanly entering PAMELA’s acceptance, may induce a signal into one or more of the AC scintillators due to backscattering from the calorimeter. Studies to discriminate backscattering events from false triggers have been performed with test-beam data and compared to simulations (Section 4). Information from the AC detectors can be implemented in a second level trigger, to reduce online the number of false triggers, and may be activated by an uplink command from ground (Lundquist et al., 2003).

2. The anticoincidence system

The anticoincidence system consists of five plastic scintillators; four of them (CAS) cover the sides of the magnet and one (CAT) covers the top of the magnet, and has a rectangular hole corresponding to the tracker acceptance (Fig. 1, right). Each CAS (CAT) scintillator is 8 mm thick and is read out by 2 (8) photomultiplier tubes (PMTs). The scintillating material is a Bicorn BC-448M cross-linked polymer, which has been chosen for its characteristics: fast response time (~ 1.5 ns), robustness, good radiation resistance and in particular good temperature stability. The thermal issue plays an important role especially during the transportation to the launch site. During flight, the experiment will run in an air-filled pressurised container, which improves heat exchange. The operational temperature for PAMELA will be kept between 5 and 40 °C by the onboard CPU. The PMTs used in the design are small-form-factor R5900U tubes, manufactured by Hamamatsu, and are operated at a constant high voltage (800 V). The 16 PMTs are connected to a read-out board, whose scheme is shown in Fig. 2. The discriminator registers an event as a ‘hit’ if the output voltage from the integrator is larger than the DAC voltage, which is user-defined, and set to ~ 0.5 mip (energy released in the

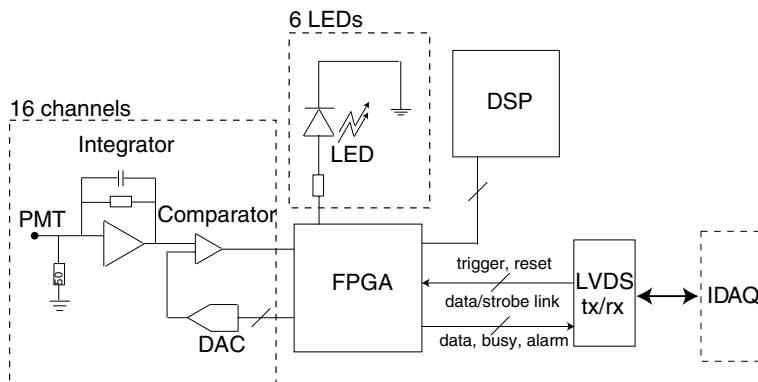


Fig. 2. Anticoincidence read-out scheme. The DSP is only used during the monitoring procedure.

detector by a minimum ionising particle) through a programmable logic device (FPGA). This action is performed independently on each channel. The AC system does not store information on the deposited energy, but only binary information whether the deposited energy is larger than ~ 0.5 mip. The FPGA reads continuously the discriminator output and stores the data in memory, in the form of a ‘shift register’, which contains information on hits on the 16 AC channels in a time window of $1.28 \mu\text{s}$, divided in 16 bits per channel (80 ns time resolution). A scintillator is hit when at least one of the 2 facing PMTs (8 for CAT) detects a particle within the $1.28 \mu\text{s}$ time window. The efficiency for all AC detectors is better than 99.9%. When a trigger arrives (from the IDAQ) to the FPGA, the shift register is ‘frozen’. In the frozen shift register, hits coincident with the trigger are registered in the central 2 bits, while the first (last) bit refers to particles interacting ~ 600 ns before (after) the trigger. The time of $1.28 \mu\text{s}$ has been chosen to allow an overlap with the calorimeter self-trigger, which is issued a few hundred of ns after the interaction of a particle.

The FPGA also has the task to communicate with the PAMELA data acquisition system (IDAQ). The communication between the FPGA and the IDAQ takes place via Low Voltage Differential Signal (LVDS) links, and consists of bidirectional data/strobe lines, trigger and other control lines. Among them, the alarm line is generated inside the FPGA and records failures in the AC electronic components (i.e., regulator failure due to SEU or latch-up, malfunctioning DSP), over-temperature conditions or errors in data transmission over the LVDS links.

3. The monitoring system

After production, the detector characteristics have been investigated in the laboratory (Orsi, 2004). At a later stage, any variation from the previously measured characteristics must be assessed during the flight. Once per orbit, on the ascending node, the data acquisition is stopped and a calibration procedure is performed. All PAMELA detectors are calibrated, sequentially and independently. The monitoring system for the PAMELA anticounters makes use of low intensity red LEDs glued onto each scintillator. Each LED emits short light pulses ($\lambda \approx 640$ nm), that reproduce mip-generated pulses inside the scintillator with respect to pulse height, shape and timescale. Since the PMT output from an LED flash *resembles*, but *is not*, the output from the interaction with a ionising particle, the procedure is referred to as monitoring and not as calibration. In order to keep the electronic design as simple as possible, the monitoring system makes use of the same electronic system used for physics operation. The FPGA drives the

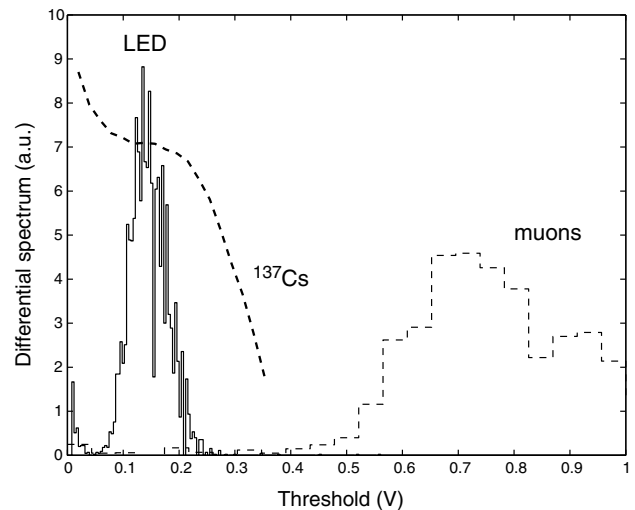


Fig. 3. Comparison between LED, ^{137}Cs and muon spectra. The x-axis, common to all data, spans the discriminator voltage range. The y-axis is linear for LEDs and muons, logarithmic for ^{137}Cs .

LEDs with a clock frequency of 40 MHz (25 ns long pulses, sent every 400 ns), while a program running on the DSP controls the whole monitoring procedure (Fig. 2). The LED-based monitoring procedure for the AC system provides large statistics in a short time. It requires less than one second to be performed and provides an integral spectrum with statistical errors of the order of 1%. The LEDs are placed far away from the PMTs, in order to provide a long path for the photons to reach the PMT, which increases the sensitivity to opacity. The LED-generated spectrum has been compared with the spectra obtained with a ^{137}Cs radioactive source and with cosmic muons (1 mip ≈ 1.6 MeV for the AC detectors). Fig. 3 shows the ^{137}Cs Compton edge at 478 keV (dotted line) and the energy released by muons in a AC scintillator (dotted histogram), compared with the LED generated spectrum (solid histogram).

4. Studies with particle beams

The response of all of the PAMELA subdetectors has been studied with particle beams on a yearly basis between 2000 and 2003. The flight AC detectors were first tested in flight-like configuration in a beam line at the SPS accelerator at CERN in September 2003, with electrons in the energy range 20–180 GeV and protons in the energy range 40–150 GeV. That beam test was also the first occasion to test with a realistic data flow the final electronic AC read-out system. The trigger to the experiment was generated by external scintillators, placed on the beam line. Beam test data has been analysed with two main aims. First, the performance of the AC electronics was studied during prolonged data acquisition runs under realistic flight conditions. Backscattering studies for the implementation of the second level trigger

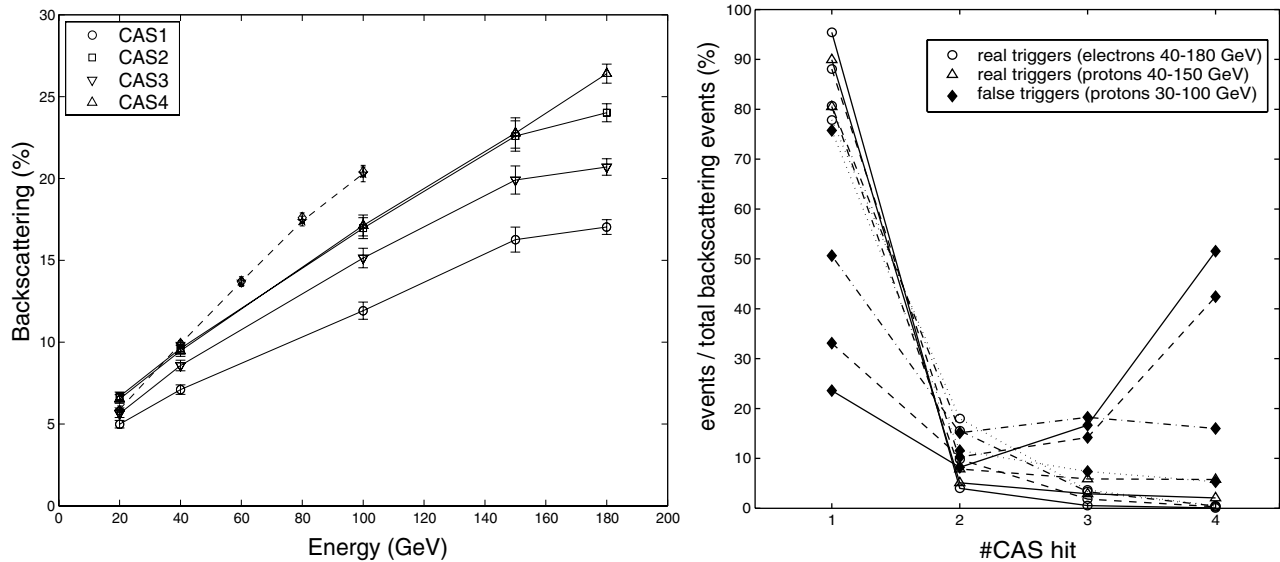


Fig. 4. (Left) Backscattering ratio versus energy for the four CAS detectors for electron beams. The dotted line refers to data from the 2001 beam test, which made use of a different experimental setup (see Section 4). (Right) The number of CAS detectors giving a signal at the same time. The figure shows the fraction of events with 1, 2, 3 or 4 CAS detectors hit, and is normalised to the number of events with activity in CAS. The data refers to backscattering events (circles and triangles) and particles impinging on the magnet (diamonds). The diamonds refer to a hit on the magnet top side through CAT (solid line), on the magnet lateral side through a side detector (dash-dot 30 GeV, dashed 100 GeV), magnet inside through S1 (dotted).

have been realised with a standalone analysis, i.e., independent of other detectors.

Almost all the beam runs consisted of particles passing cleanly through the tracker cavity, i.e., ‘good-triggers’. A significant fraction of these good events had activity in the AC system, due to backscattered particles from the calorimeter. The backscattering ratio is defined as the number of events with AC activity due to backscattering/total events. The dependence of the backscattering ratio on the hit point and on particle type and energy has been evaluated for selected runs. Fig. 4 (left) shows, for each CAS, the backscattering ratio for electrons in the energy range 20–180 GeV. The 4 solid lines refer to data from the 4 CAS detectors from the 2003 beam test. The 4 CAS detectors show a systematic difference in the backscattering ratio, due to the position of the beam, displaced from the geometrical centre of PAMELA acceptance. The dotted line refers to experimental and simulated data from the 2001 beam test, shown for reference. In 2001 the magnet was not present, which resulted in a larger backscattering ratio, due to low energy photons reaching the AC detectors without interacting in the magnet.

In an online implementation of a second level trigger which makes use of AC data on a veto basis, these good events (more than 20% at ~ 180 GeV) would be discarded. This loss is referred to as ‘self-veto’. It is thus important to distinguish between false triggers and

backscattering events. A promising method based on the multiplicity of the hits in the CAS detectors is illustrated in Fig. 4 (right). The figure shows the distribution of hits in the CAS detectors, normalised to the number of events with activity in at least one CAS detector. In the majority of ‘self-veto’ events (circles and triangles) there is activity only in one CAS, while ‘false triggers’ (particle beam impinging on the magnet) are characterised by activity in more CAS detectors.

References

- Adriani, O. et al. Nucl. Phys. B-Proc. Sup. 125, 308–312, 2003.
- Boezio, M. et al. Nucl. Instr. Meth. Phys. Res. A487, 407–422, 2002.
- Boezio, M. et al. Nucl. Phys. B-Proc. Sup. 134, 39–46, 2004.
- Cafagna, F., et al. In: Proceedings of the 28th ICRC, Tsukuba, Japan, vol. 1, 2121, 2003.
- Campana, D., et al. In: Proceedings of the 28th ICRC, Tsukuba, Japan, vol. 1, 2141, 2003.
- Lund, J. A Study of the PAMELA Anticoincidence System, KTH, Stockholm 2002. Available online at: <<http://www.particle.kth.se>> (licentiate thesis, ISBN 91-7283-314-9).
- Lundquist, J., et al. In: Proceedings of the 28th ICRC, Tsukuba, Japan, vol. 1, 2133, 2003.
- Orsi, S. The Anticoincidence Shield of the PAMELA Satellite Experiment, KTH, Stockholm 2004. Available online at: <<http://www.particle.kth.se>> (licentiate thesis, ISBN 91-7283-818-3).
- Osteria, G. et al. Nucl. Instr. Meth. Phys. Res. A518, 161–163, 2004.
- Pearce, M., et al. In: Proceedings of the 28th ICRC, Tsukuba, Japan, vol. 1, p. 2125, 2003.